Oil Weathering after the Deepwater Horizon Disaster Led to the Formation of Oxygenated Residues

ARTICLE *in* ENVIRONMENTAL SCIENCE & TECHNOLOGY · JULY 2012

Impact Factor: 5.33 · DOI: 10.1021/es3015138 · Source: PubMed

8 AUTHORS, INCLUDING:

Christoph Aeppli
Bigelow Laboratory for Ocean Sciences
24 PUBLICATIONS **358** CITATIONS
SEE PROFILE

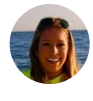

Catherine A Carmichael
Woods Hole Oceanographic Institution
18 PUBLICATIONS **410** CITATIONS
SEE PROFILE

Robert K Nelson
Woods Hole Oceanographic Institution
102 PUBLICATIONS **2,339** CITATIONS
SEE PROFILE

Christopher M Reddy
Woods Hole Oceanographic Institution
213 PUBLICATIONS **6,084** CITATIONS
SEE PROFILE

Environmental Science & Technology

Article

pubs.acs.org/est

Oil Weathering after the *Deepwater Horizon* Disaster Led to the Formation of Oxygenated Residues

Christoph Aeppli,*[,†] Catherine A. Carmichael,[†] Robert K. Nelson,[†] Karin L. Lemkau,[†] William M. Graham,[‡] Molly C. Redmond,[§] David L. Valentine,[§] and Christopher M. Reddy[†]

[†]Department of Marine Chemistry & Geochemistry, Woods Hole Oceanographic Institution, Woods Hole, Massachusetts 02543, United States

[‡]Department of Marine Science, University of Southern Mississippi, Hattiesburg, Mississippi 39529, United States

[§]Department of Earth Science and Marine Science Institute, University of California—Santa Barbara, Santa Barbara, California 93106, United States

Supporting Information

ABSTRACT: Following the *Deepwater Horizon* disaster, the effect of weathering on surface slicks, oil-soaked sands, and oil-covered rocks and boulders was studied for 18 months. With time, oxygen content increased in the hydrocarbon residues. Furthermore, a weathering-dependent increase of an operationally defined oxygenated fraction relative to the saturated and aromatic fractions was observed. This oxygenated fraction made up >50% of the mass of weathered samples, had an average carbon oxidation state of −1.0, and an average molecular formula of $(C_5H_7O)_n$. These oxygenated hydrocarbon residues were devoid of natural radiocarbon, confirming a fossil source and excluding contributions from recent photosynthate. The incorporation of oxygen into the oil's hydrocarbons, which we refer to as oxyhydrocarbons, was confirmed from the detection of hydroxyl and carbonyl functional groups and the identification of long chain (C_{10}–C_{32}) carboxylic acids as well as alcohols. On the basis of the diagnostic ratios of alkanes and polycyclic aromatic hydrocarbons, and the context within which these samples were collected, we hypothesize that biodegradation and photooxidation share responsibility for the accumulation of oxygen in the oil residues. These results reveal that molecular-level transformations of petroleum hydrocarbons lead to increasing amounts of, apparently recalcitrant, oxyhydrocarbons that dominate the solvent-extractable material from oiled samples.

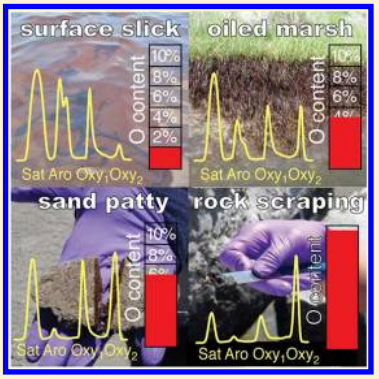

INTRODUCTION

The explosion of the *Deepwater Horizon* oil drilling rig in the Mississippi Canyon block 252, Gulf of Mexico on April 20, 2010 resulted in the release of an estimated 5.3×10^8 kg of oil and 1.7×10^8 kg of gas from the Macondo well (MW),[1−3] making it the largest marine spill in US history.[4] An additional 8.2×10^6 L of the dispersants Corexit 9500 and 9527 were collectively applied in the subsurface and at the ocean surface.[5] Numerous studies detected deep plumes of water enriched with hydrocarbons, including gases and water-soluble components of the oil and dispersants.[2,5−10] Extensive biodegradation of the gas occurred within this plume,[8,10−13] however, approximately $9 \pm 4 \times 10^7$ kg of hydrocarbons formed surface slicks[2,3] that oiled >1000 km of beaches in the Gulf of Mexico.[14,15]

In contrast to the fate of gas in the water column, the character, fate, and compositional changes of the surface slicks in the Gulf of Mexico have received limited attention.[16,17] Although the slicks disappeared within weeks of capping the MW, and in spite of extensive cleanup activities along the affected beaches, oil-soaked sands have continued to wash ashore.[15] Elevated levels of petroleum hydrocarbons were detected in coastal waters[18] and saltmarsh sediments.[19]

When investigating the fate and transport of hydrocarbons from the MW, these studies have focused on compounds amenable to separation by gas chromatography (GC), i.e., PAHs, normal alkanes, select iso-, cyclo-, and branched alkanes, and hopane and sterane biomarkers. But for the MW oil, these traditional analytes account for less than 25% of the oil mass,[2] underscoring current analytical limitations for studying oil spills. In addition, evidence from field[20−23] and laboratory studies[24−26] indicates that compounds can be formed from weathering, most of which are not targeted compounds in spill studies or are not amenable to GC. For example, one laboratory study showed an increase in oxygen content along with a relative decrease in aromatic and saturated compounds upon photooxidation of weathered light crude oil.[25] Similarly, extracts of oil and bitumen with varying degrees of weathering showed an increasing oxygen content (up to 10% oxygen by mass, with no concurrent increase in N and S), the formation of carboxylic acids, ketones, and esters, and a diminished saturated and

Received: April 17, 2012
Revised: July 13, 2012
Accepted: July 18, 2012
Published: July 18, 2012

aromatic content upon weathering.[23] These studies indicate that oil weathering can lead to oxygenation. We sought to use the *Deepwater Horizon* disaster to study oxygenation of oil undergoing natural weathering processes such as dissolution, evaporation, biodegradation, and photooxidation.

The molecular complexity of crude oil presumably translates to a similar complexity for oxygenated molecules derived from the components of crude oil, but such a determination is hampered by the lack of analytical tools available to identify and quantify individual components of complex mixtures. Instead, oxygenated components of crude oil are typically binned into bulk fractions, empirically defined by solubility or through liquid chromatography. Thus, discussions on these oxygenated fractions of crude oil, or its distilled products, can be confusing because of the lack of molecular specificity and the empirical nature of the binned fractions. For example, the oxygenated residues resulting from weathering could be considered a *polar fraction* but would be distinct from the resins, asphaltenes and nitrogen, sulfur, and oxygen (NSO) compounds found in native crude oils that share some similar properties and are commonly referred to by the same term. In addition, the term *polar* is used in multiple ways in oil spill science: it can refer to water solubility (e.g., naphthalene relative to other PAHs); retardation on silica gel in column or planar liquid chromatography, low volatility hence being retained in gas chromatography (i.e., not GC-amenable), or precipitation in some organic solvents, such as hexane (Table S3 of the Supporting Information, SI). Because of these ambiguities, we avoid the term *polar fraction* for describing oxygenated components of oil, and instead use the term *oxygenated fraction* in reference to our operationally defined separations, and *oxyhydrocarbons* to refer to those compounds that form from the oxygenation of hydrocarbons.

The two primary goals of this research were to use samples collected after the *Deepwater Horizon* disaster (i) to study systematic changes in the operationally defined saturate (F_{Sat}), aromatic (F_{Aro}), and oxygenated (F_{Oxy1}, F_{Oxy2}) fractions during natural weathering of the MW oil and (ii) to identify the processes responsible for observed changes. Using bulk and molecular techniques, we analyzed samples at different stages of weathering during an 18-month period following the initiation of the spill. These samples included the MW oil,[2] sea surface oil slicks, oil-soaked sands ("sand patties") and oil-covered rocks ("rock scrapings") collected from impacted beaches. We focused on the characteristics and fate of the F_{Oxy1} and F_{Oxy2} (collectively F_{Oxy1+2}) fractions, as defined by thin layer chromatography–flame ionization detection (TLC–FID). We show that with increasing weathering F_{Oxy1+2} in samples increased concurrently with decreases in F_{Sat} and F_{Aro}.

MATERIALS AND METHODS

Sampling and Sample Extraction. A total of 146 samples were collected over an 18-month period. The sampling locations are depicted in Figure 1. The samples include the MW oil, surface slicks collected from May to June 2010 (including oil scraped off freshly oiled marsh grasses and *Deepwater Horizon* debris[16]), as well as sand patties and rock scrapings collected from July 2010 to November 2011. The samples were stored in the dark at 4 °C until analysis. Constant *n*-alkane distributions and ratios of *n*-octadecane (*n*-C_{18}) to phytane of control samples extracted at different times of storage (days up to four months) indicated no oil degradation occurred during storage. See Table S1 and Figure S1 (SI) for coordinates, collection times, and representative images of the samples.

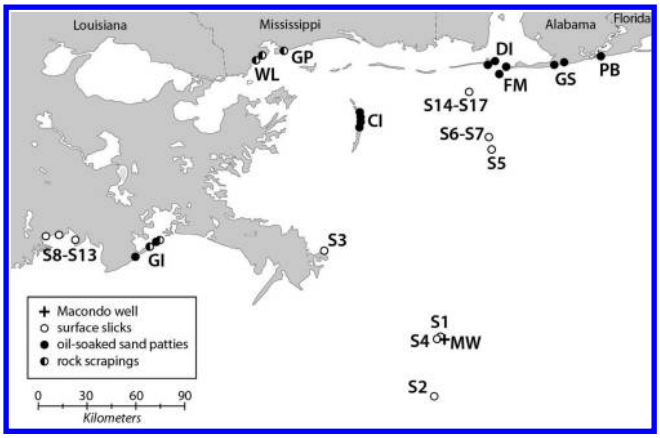

Figure 1. Overview of collected samples. The surface slicks (S1–S17) are specifically labeled. For the sand patties (B1–B95) and rock scrapings (R1–R18), only the general locations are indicated: Perdido Beach, FL (PB), Gulf Shores, AL (GS), Fort Morgan, AL (FM), Dauphin Island, AL (DI), Gulf Port, MS (GP), Waveland, MS (WL) Chandeleur Islands, LA (CI), Grand Isle, LA (GI). See Table S1 of the SI for detailed sampling locations and dates.

The MW oil and surface slick samples were dissolved in dichloromethane (DCM) at concentrations of 10 to 50 mg material mL^{-1}. The sand patties and rock scrapings (1 to 5 g) were extracted in glass centrifuge tubes three times with 10 mL of DCM/methanol (80/20), by vigorously shaking, centrifuging (1600 rpm for 5 min), and collecting the combined extracts. The combined extracts were dried with Na_2SO_4 and used for further analysis. The fraction of solvent-extractable material in the sand patties was gravimetrically determined. The moisture content was separately determined gravimetrically by drying aliquots of samples (24 h at 60 °C).

Isolation of Saturated, Aromatic, and Oxygenated Fractions. F_{Sat}, F_{Aro}, F_{Oxy1}, and F_{Oxy2} of select samples (samples MW, S4, B47, B65; see Table S1 of the SI) were isolated using silica-gel flash column chromatography (10 g 200–400 mesh silica gel, 20 mL 1 cm i.d. glass column). Sample aliquots (~100 mg extract in DCM) were loaded on to a column to successively isolate the F_{Sat} (eluted with 50 mL *n*-hexane), F_{Aro} (50 mL *n*-hexane/DCM 70/30), F_{Oxy1} (30 mL DCM/methanol 97/3), and F_{Oxy2} (50 mL DCM/methanol 80/20). The recovery of the combined fractions was 80 to 95%. We checked the purity of the isolates by analyzing the individual fractions using TLC–FID, described below. These isolated fractions were used for further analysis (see below).

Analytical Methods. The amount of saturated, aromatic, and oxygenated fractions in extracts was quantified using a TLC–FID analyzer (Iatroscan MK-5, Iatron Laboratories, Tokyo, Japan).[24,27] Briefly, 1 to 5 μL of sample extracts (in DCM or DCM/methanol) were spotted on the base of a silica-gel sintered glass rod (Chromarod S III, Iatron Laboratories) and successively developed in hexane (26-min development time), toluene (12 min), and DCM/methanol 97/3 (5 min). Between each development, the rods were dried for 1 min at 500 mbar and 70 °C. Rods were analyzed in the TLC–FID analyzer using a 30 sec scan time with the FID operating at a flow of 2 L min^{-1} air and 160 mL min^{-1} H_2. Four distinct peaks were observed, which we operationally defined, in order of least retention, as saturated (F_{Sat}), aromatic (F_{Aro}), oxygenated 1

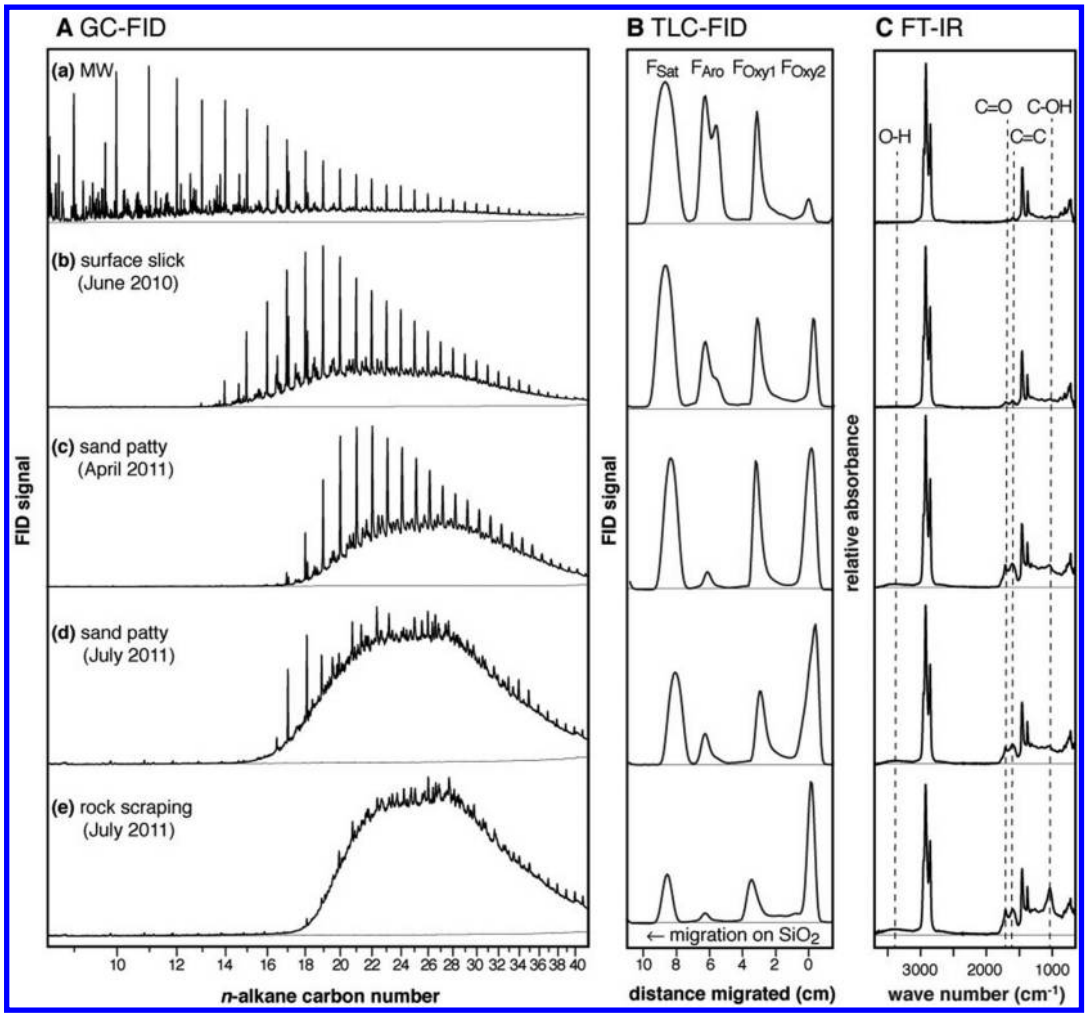

Figure 2. (A) GC−FID, (B) TLC−FID, and (C) FT−IR traces of (a) MW oil, (b) surface slick S4, (c) sand patty B47 collected at CI, (d) sand patty B65 collected at GS, and (e) rock scraping R11 collected at GI. The MW oil, slick, and scrapings were dissolved in DCM, while the sand patties are the analysis of the whole extract via solvent extraction (DCM/methanol 90/10). Similar maximal TLC−FID signal intensities were obtained for all samples (5−15 mV).

(F_{Oxy1}), and oxygenated 2 (F_{Oxy2}) fractions. This elution scheme was verified with known saturated and aromatic compounds (n-C_{16} and chrysene); for the F_{Oxy1+2}, we used model compounds (2-hexadecanone, 2-hexadecanol, hexadecanoic acid, methyl pentadecanoate, and 9,10-dihydroxy octadecanoic acid; Figure S2 of the SI). As F_{Oxy2} is retained on the TLC rods with our method, it is difficult to determine the true spectrum of compounds in this fraction. Note that we observed hexadecanoic acid and 9,10-dihydroxy octadecanoic acid eluting in the windows of F_{Oxy1} and F_{Oxy2}, respectively. The results are reported as relative peak areas of these fractions. These relative peak areas agreed with the masses of F_{Sat}, F_{Aro}, F_{Oxy1}, and F_{Oxy2} of selected samples isolated by silica gel column chromatography (see above). Blank analyses of rods were devoid of any detectable signal. The TLC−FID response was linear for total peak areas between 200 − 600 mV·s, and we varied the sample size to operate within this range.

To test the long-term reproducibility of this method, we analyzed one sand patty extract 47 times over a period of five weeks, resulting in 39.8 ± 1.5, 5.1 ± 0.5, 21.9 ± 1.8 and 33.2 ± 2.1% for the F_{Sat}, F_{Aro}, F_{Oxy1}, and F_{Oxy2}, respectively (uncertainties as 1σ standard deviation); the relative standard deviations were therefore <10% for all four fractions. While we know of no standard reference materials for TLC−FID of oils, especially weathered oils, our results were consistent with analysis of MW oil by two external laboratories that used TLC−FID and liquid chromatography.[2] During the TLC−FID analytical procedure, compounds with boiling points below n-pentadecane (n-C_{15}) are lost.[28] We corrected the TLC−FID fractions for the mass loss of these low-boiling compounds (determined by GC−FID and simulated distillation; see SI for calculation). The correction was only significant for the MW oil and some surface slick samples, as no low-boiling compounds were present within sand patties and rock scrapings.

GC−FID analysis of extracts was performed on a Hewlett-Packard 5890 Series II GC. Samples (10 to 50 mg mL^{-1} DCM/methanol solution), spiked with perdeuterated n-C_{16} as an internal standard, were injected (1 μL injection volume) in splitless mode, and separated on a Restek Rtx-1 capillary column (30 m, 0.25 mm I.D., 0.25 μm film) with 5 mL min^{-1} H_2 as the carrier gas. The temperature program was 7 min at 35 °C, ramped to 315 at 6 °C min^{-1} and to 320 at 20 °C min^{-1} (held 15 min). Total petroleum hydrocarbons (TPHs) were quantified by integrating the total area of the FID signal, using DCM-blank subtraction and response factors determined from n-alkane standards. Ratios of n-C_{18} and phytane were

dx.doi.org/10.1021/es3015138 | Environ. Sci. Technol. 2012, 46, 8799−8807

determined by integrating the corresponding peaks. For each sample, the GC-amenable fraction was calculated as the TPHs content divided by the mass of the solvent-extractable material.

PAH concentrations from selected samples were measured by Alpha Analytical (Mansfield, MA), using a modified EPA 8270 method.[2,16] Additional PAH and hopane analyses were performed using GC−mass spectrometry (GC−MS; Agilent 6890 GC with a 5973 MSD), 1 μL sample injection (splitless) using He (10.5 psi constant pressure) as carrier gas and the following GC temperature program: 4 min at 40 °C and ramped to 320 at 5 °C min^{-1} (held 15 min). The following mass traces were recorded in single ion monitoring mode: m/z 178, 192, 206, and 220 (for C_0, C_1, C_2, and C_3-phenanthrene isomers), m/z 228, 242, 256, and 270 (for C_0, C_1, C_2, and C_3-chrysenes), and m/z 191 (for hopanes). Compound ratios agreed with those obtained by Alpha Analytical.

Elemental analysis (for C, H, N, O, and S content) of the MW oil, surface slicks, solvent-free extracts from sand patties and rock scrapings, and selected isolated fractions from silica gel column chromatography was performed by Midwest Microlabs (Indianapolis, IN).

The natural radiocarbon (^{14}C) content and stable carbon isotope ratios of the whole extract and isolates of all four fractions (F_{Sat}, F_{Aro}, F_{Oxy1}, and F_{Oxy2}) of two representative sand patty samples B47 and B65 was measured at the National Ocean Sciences Accelerator Mass Spectrometry (NOSAMS) facility in Woods Hole, MA.[29] All ^{14}C measurements are expressed as fraction modern (f_M) and $\Delta^{14}C$. For reference, fossil carbon and recently photosynthesized carbon have f_M of 0 and 1.0, respectively (we chose a f_M of 1 for the ^{14}C content of dissolved inorganic carbon for coastal waters of the Gulf of Mexico). Using $\Delta^{14}C$ nomenclature, petroleum and recently photosynthesized carbon have values of −1000 and 0‰, respectively.

Comprehensive two-dimensional GC (GC × GC) analysis of biomarker ratios was performed on GC × GC−FID and GC × GC−MS systems according to previously published procedures.[16,30] Fourier transform infrared spectroscopy (FT−IR) was performed by Infrared Interpretations (Naugatuck, CT). ^1H NMR analysis of samples dissolved in $CDCl_3$ was conducted on a Bruker 400 MHz NMR spectrometer.

Select whole extracts and isolated fractions were silylated for GC−MS and GC × GC−MS analysis. Silylation was performed by reacting (1 h at 70 °C) 5 to 50 mg oil sample (in 50:50 DCM: *N,O*-bis(trimethylsilyl) trifluoroacetamide containing 1% trimethylchlorosilane). Alternatively, select extracts (in diethyl ether) were methylated for 1 h at 0 °C with in situ generated diazomethane from the hydrolysis of *N*-methyl-*N*-nitroso-*p*-toluenesulfonamide.

RESULTS AND DISCUSSION

Weathering of the Saturates and Aromatics. A set of 146 samples collected over 18 months was analyzed to study weathering of the MW oil as it traveled from the seafloor, through the water column, surfaced as oil slicks, and reached the beaches (Figure 1). Figure S1 of the SI displays representative pictures of the different sample types. To confirm their origin, 58 samples were fingerprinted by GC × GC−FID using published hopane and sterane biomarker ratios.[16] These samples were representative of the larger sample set, as the other 88 samples were situated nearby and had a similar appearance (color, size, and shape). Fifty-four matched the MW oil. The nonmatch of four samples was not surprising, as they belonged to a set of 15 nonsandy, asphalt-like samples found at location GI and CI (Figure 1) that were visually and physically distinct from the other sample types in this study. These samples were excluded from further consideration.

With increasing time and distance traveled, samples showed typical signs of weathering, as observed in their GC−FID chromatograms (Figure 2A). Most surface slicks collected up to 240 km from the Macondo well showed losses of compounds eluting earlier than n-C_{13}, consistent with evaporative loss. In addition, dissolution appears to be affecting these samples, indicated by the depletion of naphthalene relative to C_1-naphthalene as compared to the MW oil (Figure S4 of the SI). Interestingly, the surface slicks S1 and S2 (collected on May 31 and June 1, 2010 respectively) contained n-alkanes smaller than n-C_{10} (Figure S3 of the SI). As atmospheric measurements during the spill implied that such compounds evaporated within hours,[9] S1 and S2 are, therefore, recently surfaced oil. These findings suggest that these samples were mainly subject to weathering processes in the water column, and hence, represent the oil composition at an early stage of surface weathering.

Although extensive biodegradation of C_1 to C_5 hydrocarbons was observed in the water column,[13] this process did not affect the longer chain alkanes in surface slicks. This is reflected by rather constant n-C_{18}/phytane ratio (2.5 to 3.0) for these samples, as compared to the MW oil (2.5; Table S1 of the SI). In contrast, samples collected on beaches between July 2010 and November 2011 showed extensive biodegradation. For example, B45 and B65 had n-C_{18}/phytane values of 2.1 and 0.1, respectively, and the rock scraping R11 lost most resolvable alkanes, indicative of severe biodegradation (Figure 2A).

We measured PAHs for a subset of 10 samples (Figure S4 of the SI). The total concentration of 30 PAHs (defined in Figure S4 of the SI) decreased from 18 mg g^{-1} oil for MW,[2] to 7.7−13 mg g^{-1} oil for surface slicks, to 0.6−2.8 mg g^{-1} extractable material for sand patties and rock scrapings. As smaller PAHs such as naphthalene and phenanthrene are more water-soluble than other PAHs, they were depleted in the surface slicks (Figure S4 of the SI). In line with this observation, these PAHs were in turn detected in mesozooplankton in the Gulf of Mexico.[31] While all of the alkylated naphthalenes were absent in sand patties and rock scrapings, chrysene and its alkylated congeners were relatively enriched in these samples compared to the MW oil; this is indicative for weathering.[32] PAH losses, calculating by normalization to $17\alpha(H),21\beta(H)$-hopane (referred to as "hopane"),[33] were 35−78% for surface slicks, 83−98% for sand patties, and 93% for the rock scraping (Figure S5 of the SI).

Increase of Oxyhydrocarbons Upon Weathering. Despite appearing rich with oil, solvent extraction of sand patties yielded only 15 ± 7% on a dry weight basis (Figure S1 of the SI). During beach cleanup efforts, this percentage should be used to ensure accurate mass balance calculations. Furthermore, we observed that only a small fraction of this extractable material could be accounted for by GC−FID analysis, with an average of only 32 ± 5% of extractable material being GC amenable (Figure S9 of the SI).

We hypothesized that the non-GC amenable fraction consists of some types of oxygenated compounds, based on findings from previous lab and field weathering studies.[23,25] This was confirmed by direct measurements of oxygen content for whole extracts, which reached up to 14% by mass as the GC-amenable fraction decreased (Figure 3a). The TLC−FID measurements

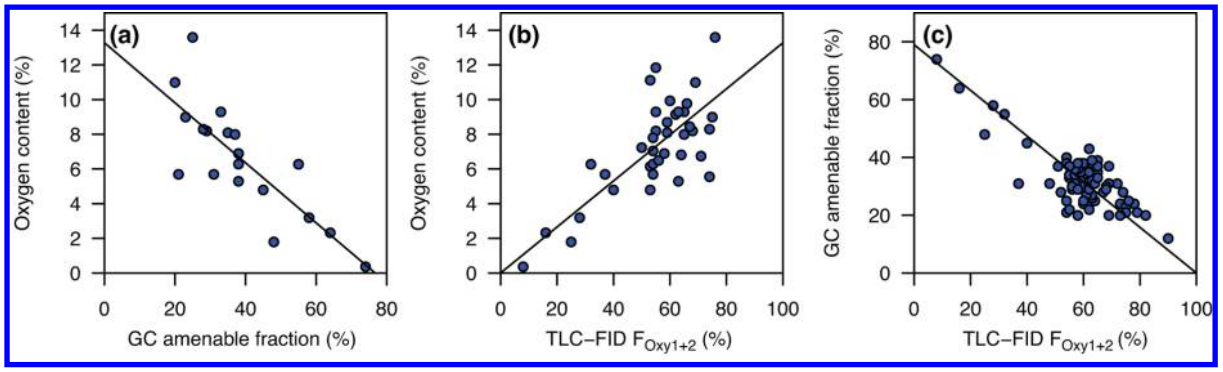

Figure 3. (a) Oxygen content of whole extracts versus the GC-amenable fraction. (b) Oxygen content of whole extracts versus the F_{Oxy1+2} detected by TLC–FID. (c) GC-amenable material versus TLC–FID measured F_{Oxy1+2} (slope = −0.79; R^2 = 0.96).

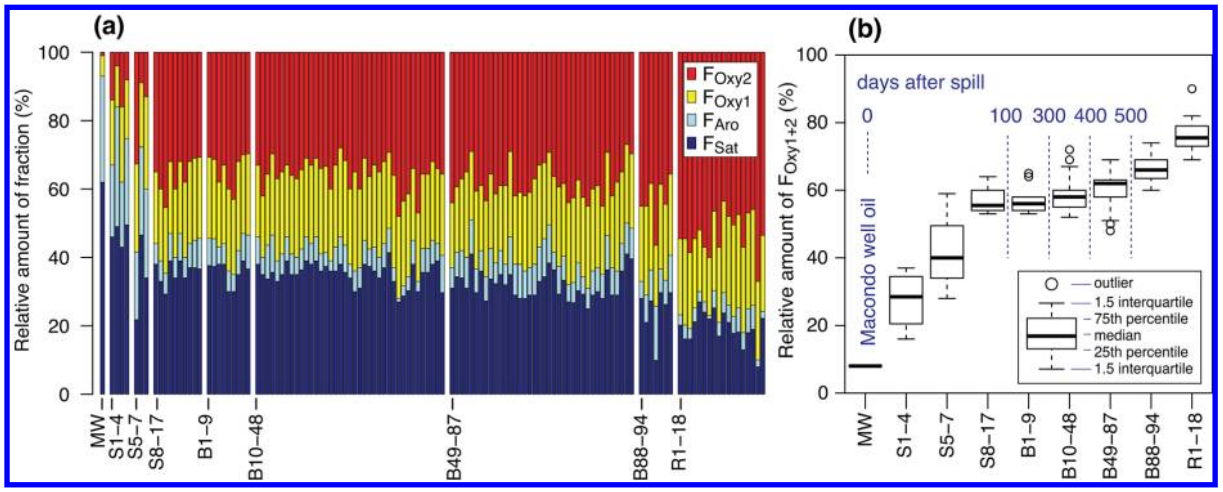

Figure 4. (a) Relative distribution of saturated (F_{Sat}), aromatic (F_{Aro}), and oxygenated (F_{Oxy1} and F_{Oxy2}) fractions in samples collected between April 2010 and November 2011, including the MW oil, fresh surface slicks (S1–4), oil-coated debris samples (S5–7), slicks recovered from marsh and shells (S8–17), oil-soaked sand patties collected July 2010 through January 2011 (B1–9), April 2011 (B10–48), July 2011 (B49–87), November 2011 (B88–94), and rock scrapings collected in July 2011 (R1–18). See Table S1 of the SI for sampling locations and dates. (b) Box plot for F_{Oxy1+2}, grouping together different sample types and collection times (the time scale in days of collection after the onset of the spill is given in blue for the surface slicks and sand patties).

also showed a concurrent increase in F_{Oxy1+2} (Figure 3b). As a result, the TLC-measured F_{Oxy1+2} negatively correlated with the GC-amenable fraction (Figure 3c), confirming that oxy-hydrocarbons populate the non-GC amenable fraction of weathered MW oil. Note that some compounds of F_{Oxy1} still might be GC amenable (e.g., ketones, alcohols, esters). However, isolates of F_{Oxy1} produced only a minor GC–FID signal. Although we recognize that different compound classes reside in F_{Oxy1} and F_{Oxy2}, we often combine these fractions into F_{Oxy1+2}.

We calculated the elemental composition of F_{Oxy1+2} from the C, H, N, O, and S elemental analysis of the whole extracts (Table S1 of the SI), assuming a fixed composition of F_{Sat} ($C_1H_{2.1}$) and F_{Aro} ($C_1H_{1.1}S_{0.1}$). The resulting average molecular formula for F_{Oxy1+2} was $C_1H_{1.4}O_{0.2}$. This indicates an average C oxidation state of −1.0, assuming that all O are bound to C.[34] The F_{Oxy1+2} was calculated to contain 13 ± 3% oxygen by mass for 37 weathered oil samples (mean ±1σ standard deviation; Figure S10 of the SI). The N and S content of F_{Oxy1+2} remained <2% for all analyzed samples, indicating no significant N or S enrichment in F_{Oxy1+2}. With such a high oxygen content for F_{Oxy1+2}, it may be considered water-soluble, but it appears to be rather the opposite. Most of our collected sand patties or rock scrapings were in contact with water for up to 18 months.

The F_{Oxy1+2} increased during oil weathering, as can be seen qualitatively from comparing GC–FID and TLC–FID traces (Figure 2A,B) from samples spanning 0 to >500 days postspill. More quantitatively, F_{Oxy1+2} correlated with the hopane normalized n-C_{18}, phytane, or chrysene concentrations (R^2 = 0.66 − 0.82; Figure S7 of the SI). As these are general weathering indicators, the correlations imply that the amount of F_{Oxy1+2} is suitable to assess degrees of weathering, especially when saturated and aromatic compounds are no longer present.

Kinetics of Oxygenation. We observed clear trends in the fractional composition of the samples during weathering (Figure 4). Early stage weathering can be seen in the fresh surface slicks S1–S4, where evaporation and water washing appear to be responsible for the increase of F_{Oxy1+2}, while F_{Aro} was still comparable to the MW oil. In contrast, oil slicks S5–S17 scraped off grass, shells, or *Deepwater Horizon* debris up to 100 days after the spill already had 57 ± 4% F_{Oxy1+2} and a significantly reduced F_{Aro}. Remarkably, the composition of these samples was not significantly different (Student's t-Test p-value = 0.15) from that of sand patties B1–B87, which were collected from June 2010 through July 2011 and had F_{Oxy1+2} of 59 ± 5%. Sand patties B88–B94 collected in November 2011 had a slightly higher F_{Oxy1+2} of 66 ± 5%, which was significantly

dx.doi.org/10.1021/es3015138 | Environ. Sci. Technol. 2012, 46, 8799–8807

different from samples B1−B87 ($p < 0.01$). Common to all sand patties was the low amount of F_{Aro} (7 ± 2%).

Interestingly, the most dramatic changes of F_{Oxy1+2} occurred during the first 100 days after the onset of the spill; thereafter, the increase in F_{Oxy1+2} proceeded slowly (Figure 4b). We also found that the formation rate of F_{Oxy1+2} is dependent on the sample type. For example, samples scraped off rocks 15 months after the spill (R1−18) had a higher amount of F_{Oxy1+2} ($p < 0.001$) compared to sand patties collected at the same time and locations (B49−87; Figure 4b). This could be explained by a presumed higher surface area-to-volume ratio for the rock samples (Figure S1 of the SI); thus, the rock scrapings faced greater solar exposure and water contact than sand patties, making them more susceptible to weathering processes.

The rapid initial formation and subsequent slow and steady increase in F_{Oxy1+2} implies that the oxygenated residues are recalcitrant rather than a short-living intermediate for complete oil mineralization. As F_{Oxy1} remained rather constant for all weathered sand patties and rock scrapings (23 ± 3%), this fraction might be intermediately formed, whereas F_{Oxy2} would contain the final products of oil weathering. From model compounds (see Methods Section), we can state that the additional of two hydroxyl groups on straight chain carboxylic acids can move a compound from the F_{Oxy1} to F_{Oxy2}. It is very likely that a stepwise oxygenation is occurring during oil weathering, thus transferring compounds from F_{Sat} and F_{Aro} via F_{Oxy1} to F_{Oxy2}. Note, however, that F_{Oxy2} can contain many different compound classes that can be further fractionated at a finer resolution with appropriate chromatographic systems.

Oxyhydrocarbons Are Newly Formed and Not Just Preferentially Enriched. One key question is whether the increase in F_{Oxy1+2} is simply preferential enrichment of F_{Oxy1+2} relative to F_{Sat} and F_{Aro}, or whether it is due to the production of oxyhydrocarbons. Enrichment occurred, but there is strong evidence that oxygenated residues were newly formed. To determine this, we normalized our TLC−FID data to hopane, a recalcitrant internal tracer.[33] This approach has been used successfully for assessing the loss of individual saturated or aromatic compounds (Figure S7 of the SI). Similarly, calculating the amount of hopane relative to the whole of GC−FID signal (which largely corresponds to F_{Sat} plus F_{Aro}; Figure 3c) shows an increasing loss of F_{Sat} plus F_{Aro} relative to hopane with progressive weathering. Concurring with this trend, samples had an increased hopane-normalized F_{Oxy1+2} value, which reached up to 17 times the value of the MW oil (Figure 5). For exclusive preferential enrichment without oxyhydrocarbon formation, the hopane-normalized F_{Oxy1+2}-value would stay at the value of the MW oil. In addition, we calculated that the oxygenation level for F_{Oxy1+2} of weathered samples is higher than that of native MW oil oxyhydrocarbons (Figure S10 of the SI). These results show that oxyhydrocarbons were newly formed during oil weathering.

Oxygenation of Oil Yields Recalcitrant Oxyhydrocarbons. To confirm if the oxygenated material was from the alteration of the spilled oil and not from recently photosynthesized carbon, we measured the radiocarbon content of whole extracts as well as isolated fractions (F_{Sat}, F_{Aro}, F_{Oxy1}, and F_{Oxy2}) of two representative sand patties. All of the fractions contained only fossil, and hence oil-derived carbon ($f_M < 0.012$ and $\Delta^{14}C < -988‰$; Table S2 of the SI). Previous studies tracing the bacterial uptake of carbon from oil spills have shown bacterial lipids containing petroleum-derived carbon.[35] It would be reasonable to assume that the oxygenated fraction in these

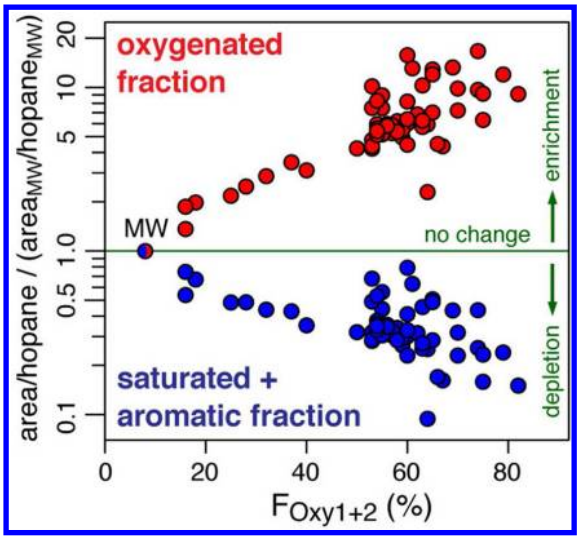

Figure 5. Ratio of TLC−FID areas of combined F_{Sat} plus F_{Aro} (blue circles) and F_{Oxy1+2} (red circles) to 17α(H),21β(H)-hopane,[35] normalized to the value of the MW oil. The green arrows and lines represent enrichment, depletion, or no change of the fractions relative to hopane. The figure shows an increase of oxyhydrocarbons relative to hopane, concurrent with a decrease in saturated and aromatic compounds.

samples also includes the oxygenated biomass of the bacteria respiring the oil. However, this seems to be a minor contribution, as shown from the carbon preference indices (CPI) of saturated long chain fatty acids (see below).

On the basis of the enhanced oxygen content of the F_{Oxy1+2} and its increase in absolute abundance, we investigated the distribution of oxygen-containing moieties in weathered oil. FT−IR analyses of selected samples reveal increase in carboxylation and hydroxylation with weathering state, as can be seen by increase in O−H, C═O, and C−O frequencies across MW oil, sand patties and rock scrapings (Figure 2C). Using ^{1}H NMR we also observed a slight increase in ester and carboxyl protons with increasing weathering (Figure S6 of the SI). Furthermore, GC × GC analysis revealed a series of C_{10} to C_{32} straight chain carboxylic acids and various alcohols in derivatized sand patty extracts that were absent in the MW oil (Figure S8 of the SI). These carboxylic acids had a CPI of 0.96, which agrees with the CPI of the *n*-alkanes in the MW oil (1.00), indicating that the acids were produced from oxidation of the oil; bacterial lipids would have a CPI of at least 2.[36] We did not quantify the derivatized compounds, but we observed a shift (10%) from F_{Oxy1} to F_{Oxy2} when whole sand patty extracts were reacted with diazomethane, indicating that more than just trace amounts were derivatized by this method.

Biodegradation and photooxidation are both likely candidates for the observed oxygenation.[37,38] The *n*-C_{18}/phytane ratios suggest progressive biodegradation with increasing F_{Oxy1+2} (Figure S7d of the SI). As further evidence for biodegradation, smaller PAHs such as phenanthrene disappeared more rapidly than chrysene (Figure S7e of the SI).[39] However, alkylated chrysene isomers were more susceptible to degradation as compared to less alkylated congeners (Figure S7f of the SI), which is indicative of photooxidation.[23,38,40] Considering the exposure of samples to water, elevated temperature and sunlight, it seems very likely that biodegradation and photooxidation both played a role for the formation of the F_{Oxy1+2}. Further support for this hypothesis is

provided by the above-discussed identification of primary alcohols and monocarboxylic acids, which are known to be typical products of biodegradation and photooxidation.[37]

Implications. Oil spill research has generally focused on saturated and aromatic compounds and overlooked oxyhydrocarbons. This study shows that oxyhydrocarbons can be a significant mass of weathered oil, and this pool of carbon should be included into mass balance considerations after oil spills. Oxyhydrocarbons are relatively persistent, potentially making them recalcitrant tracers that could be used to assess degrees and kinetics of weathering, or for oil spill forensics, especially at weathering stages when other traditionally used oil compounds are degraded.

Oxyhydrocarbons also have the potential to exhibit toxic effects. Interestingly, recent toxicological studies suggest oil compounds other than PAHs are necessary to explain observed toxicity of oil: for example, toxicity has been attributed to oil-derived carboxylic acids,[41] resins in crude oil,[42] to compounds containing hydroxyl, keto, and nitro groups extracted from oil-contaminated sediments, [43] or to uncharacterized oil weathering products.[44,45] Toxicity is often assumed to decrease during oil weathering. This is because bioavailability, which is a prerequisite for compounds to manifest toxic effect, usually negatively correlates with hydrophobicity, and because less hydrophobic saturated and aromatic compounds disappear during oil weathering.[46] However, oxygenation of oil residues during natural weathering has been suggested to increase their hydrophobicity,[23] potentially making these residues more bioavailable.

More rigorous characterization of the resulting oxyhydrocarbons coupled with toxicological assays are necessary before new conclusions about toxicity of oil weathering products can be made. Many oxyhydrocarbons are outside traditional GC analytical windows, but characterization could be achieved by direct immersion ionization techniques together with ultra high resolution MS such as Fourier transform ion cyclotron resonance mass spectrometry (FT−ICR MS). This is a promising approach for overcoming the limitations of GC-based analysis, and has been proven applicable for analyzing crude oil resins and asphaltenes.[47,48]

Overall, the results of this study pave the way for more detailed molecular and toxicological studies of oxyhydrocarbons from acute and chronic release of petroleum. In addition, this study highlights the need to continue expanding analytical method in order to understand the fate of oil and its abiotic and biotic transformation products.

■ ASSOCIATED CONTENT

Supporting Information

Supporting Figures S1−S10 and Tables S1−S3. This material is available free of charge via the Internet at http://pubs.acs.org.

■ AUTHOR INFORMATION

Corresponding Author

*Phone: (508)289-3698; e-mail: caeppli@whoi.edu.

Notes

The authors declare no competing financial interest.

■ ACKNOWLEDGMENTS

This research was made possible in part by grants from the NSF (OCE-0960841, RAPID OCE-1043976, RAPID OCE-1042097, EAR-0950600, OCE-0961725), and in part by a grant from BP/the Gulf of Mexico Research Initiative (GoMRI-015 and GoMRI-008) and the Deep-C consortium. C.A. acknowledges a Swiss National Science Foundation Postdoctoral Fellowship (PA00P2_134124). The authors wish to thank: Carl Johnson, Sean Sylva, Bryan James, Blake Hallisay, and Rainer Lohmann, and the staff at Southeast Louisiana National Wildlife Refuge for their assistance.

■ REFERENCES

(1) McNutt, M. K.; Camilli, R.; Crone, T. J.; Guthrie, G. D.; Hsieh, P. A.; Ryerson, T. B.; Savas, O.; Shaffer, F. Review of flow rate estimates of the *Deepwater Horizon* oil spill. *Proc. Natl. Acad. Sci. U.S.A.* **2011**, DOI: 10.1073/pnas.1112139108.

(2) Reddy, C. M.; Arey, J. S.; Seewald, J. S.; Sylva, S. P.; Lemkau, K. L.; Nelson, R. K.; Carmichael, C. A.; McIntyre, C. P.; Fenwick, J.; Ventura, G. T.; Van Mooy, B. A. S.; Camilli, R. Composition and fate of gas and oil released to the water column during the *Deepwater Horizon* oil spill. *Proc. Natl. Acad. Sci. U.S.A.* **2012**, DOI: 10.1073/pnas.1101242108.

(3) Ryerson, T. B.; Camilli, R.; Kessler, J. D.; Kujawinski, E. B.; Reddy, C. M.; Valentine, D. L.; Atlas, E.; Blake, D. R.; de Gouw, J.; Meinardi, S.; Parrish, D. D.; Peischl, J.; Seewald, J. S.; Warneke, C. Chemical data quantify *Deepwater Horizon* hydrocarbon flow rate and environmental distribution. *Proc. Natl. Acad. Sci. U.S.A.* **2012**, DOI: 10.1073/pnas.1110564109.

(4) Atlas, R. M.; Hazen, T. C. Oil biodegradation and bioremediation: A tale of the two worst spills in U.S. history. *Environ. Sci. Technol.* **2011**, *45* (16), 6709−6715.

(5) Kujawinski, E. B.; Soule, M. C. K.; Valentine, D. L.; Boysen, A. K.; Longnecker, K.; Redmond, M. C. Fate of dispersants associated with the *Deepwater Horizon* oil spill. *Environ. Sci. Technol.* **2011**, *45* (4), 1298−1306.

(6) Camilli, R.; Reddy, C. M.; Yoerger, D. R.; Van Mooy, B. A. S.; Jakuba, M. V.; Kinsey, J. C.; McIntyre, C. P.; Sylva, S. P.; Maloney, J. V. Tracking hydrocarbon plume transport and biodegradation at *Deepwater Horizon*. *Science* **2010**, *330* (6001), 201−204.

(7) Joye, S. B.; MacDonald, I. R.; Leifer, I.; Asper, V. Magnitude and oxidation potential of hydrocarbon gases released from the BP oil well blowout. *Nat. Geosci.* **2011**, *4* (3), 160−164.

(8) Kessler, J. D.; Valentine, D. L.; Redmond, M. C.; Du, M.; Chan, E. W.; Mendes, S. D.; Quiroz, E. W.; Villanueva, C. J.; Shusta, S. S.; Werra, L. M.; Yvon-Lewis, S. A.; Weber, T. C. A persistent oxygen anomaly reveals the fate of spilled methane in the deep Gulf of Mexico. *Science* **2011**, *331* (6015), 312−315.

(9) Ryerson, T. B.; Aikin, K. C.; Angevine, W. M.; Atlas, E. L.; Blake, D. R.; Brock, C. A.; Fehsenfeld, F. C.; Gao, R. S.; de Gouw, J. A.; Fahey, D. W.; Holloway, J. S.; Lack, D. A.; Lueb, R. A.; Meinardi, S.; Middlebrook, A. M.; Murphy, D. M.; Neuman, J. A.; Nowak, J. B.; Parrish, D. D.; Peischl, J.; Perring, A. E.; Pollack, I. B.; Ravishankara, A. R.; Roberts, J. M.; Schwarz, J. P.; Spackman, J. R.; Stark, H.; Warneke, C.; Watts, L. A. Atmospheric emissions from the *Deepwater Horizon* spill constrain air-water partitioning, hydrocarbon fate, and leak rate. *Geophys. Res. Lett.* **2011**, *38*, L07803.

(10) Valentine, D. L.; Kessler, J. D.; Redmond, M. C.; Mendes, S. D.; Heintz, M. B.; Farwell, C.; Hu, L.; Kinnaman, F. S.; Yvon-Lewis, S.; Du, M.; Chan, E. W.; Garcia Tigreros, F.; Villanueva, C. J. Propane respiration jump-starts microbial response to a deep oil spill. *Science* **2010**, *330* (6001), 208−211.

(11) Hazen, T. C.; Dubinsky, E. A.; DeSantis, T. Z.; Andersen, G. L.; Piceno, Y. M.; Singh, N.; Jansson, J. K.; Probst, A.; Borglin, S. E.; Fortney, J. L.; Stringfellow, W. T.; Bill, M.; Conrad, M. E.; Tom, L. M.; Chavarria, K. L.; Alusi, T. R.; Lamendella, R.; Joyner, D. C.; Spier, C.; Baelum, J.; Auer, M.; Zemla, M. L.; Chakraborty, R.; Sonnenthal, E. L.; D'Haeseleer, P.; Holman, H.-Y. N.; Osman, S.; Lu, Z.; Van Nostrand, J. D.; Deng, Y.; Zhou, J.; Mason, O. U. Deep-sea oil plume enriches indigenous oil-degrading bacteria. *Science* **2010**, *330* (6001), 204−208.

(12) Redmond, M. C.; Valentine, D. L. Natural gas and temperature structured a microbial community response to the *Deepwater Horizon*

oil spill. *Proc. Natl. Acad. Sci. U.S.A.* **2011**, DOI: 10.1073/pnas.1108756108.
(13) Valentine, D. L.; Mezic, I.; Macesic, S.; Crnjaric-Zic, N.; Ivic, S.; Hogan, P. J.; Fonoberov, V. A.; Loire, S. Dynamic autoinoculation and the microbial ecology of a deep water hydrocarbon eruption. *Proc. Natl. Acad. Sci. U.S.A.* **2012**, DOI: 10.1073/pnas.1108820109.
(14) Graham, B.; Reilly, W. K.; Beinecke, F.; Boesch, D. F.; Garcia, T. D.; Murray, C. A.; Ulmer, F. *Deep Water: The Gulf Oil Disaster and the Future of Offshore Drilling*. Report to the President: National Commission on the BP Deepwater Horizon Oil Spill Offshore Drilling: 2011; ISBN 978−0-16−087371−3.
(15) *Summary Report for Fate and Effects of Remnant Oil in the Beach Environment*; Operational Science Advisory Team (OSAT-2), Gulf Coast Indicent Management Team: 2011; http://www.restorethegulf.gov/sites/default/files/u316/OSAT-2 Report no ltr.pdf.
(16) Carmichael, C. A.; Arey, J. S.; Graham, W. M.; Linn, L. J.; Lemkau, K. L.; Nelson, R. K.; Reddy, C. M. Floating oil-covered debris from *Deepwater Horizon*: Identification and application. *Environ. Res. Let.* **2012**, *7*, 015301.
(17) Edwards, B. R.; Reddy, C. M.; Camilli, R.; Carmichael, C. A.; Longnecker, K.; Van Mooy, B. A. S. Rapid microbial respiration of oil from the *Deepwater Horizon* spill in offshore surface waters of the Gulf of Mexico. *Environ. Res. Let.* **2011**, *6* (3), 035301.
(18) Allan, S. E.; Smith, B. W.; Anderson, K. A. Impact of the *Deepwater Horizon* oil spill on bioavailable polycyclic aromatic hydrocarbons in gulf of Mexico coastal waters. *Environ. Sci. Technol.* **2012**, *46* (4), 2033−2039.
(19) Natter, M.; Keevan, J.; Wang, Y.; Keimowitz, A. R.; Okeke, B. C.; Son, A.; Lee, M.-K. Level and degradation of *Deepwater Horizon* spilled oil in coastal marsh sediments and pore-water. *Environ. Sci. Technol.* **2012**, *46* (11), 5744−5755.
(20) Tjessem, K.; Aaberg, A. Photochemical transformation and degradation of petroleum residues in the marine environment. *Chemosphere* **1983**, *12*, 1373−1394.
(21) Burns, K. A. Evidence for the importance of including hydrocarbon oxidation-products in environmental assessment studies. *Mar. Pollut. Bull.* **1993**, *26* (2), 77−85.
(22) Ehrhardt, M. G.; Burns, K. A. Hydrocarbons and related photooxidation products in Saudi-Arabian Gulf coastal waters and hydrocarbons in underlying sediments and bioindicator bivalves. *Mar. Pollut. Bull.* **1993**, *27*, 187−197.
(23) Charrié-Duhaut, A.; Lemoine, S.; Adam, P.; Connan, J.; Albrecht, P. Abiotic oxidation of petroleum bitumens under natural conditions. *Org. Geochem.* **2000**, *31* (10), 977−1003.
(24) Garrett, R. M.; Pickering, I. J.; Haith, C. E.; Prince, R. C. Photooxidation of crude oils. *Environ. Sci. Technol.* **1998**, *32* (23), 3719−3723.
(25) Maki, H.; Sasaki, T.; Harayama, S. Photo-oxidation of biodegraded crude oil and toxicity of the photo-oxidized products. *Chemosphere* **2001**, *44* (5), 1145−1151.
(26) Fernandez-Varela, R.; Gomez-Carracedo, M. P.; Fresco-Rivera, P.; Andrade, J. M.; Muniategui, S.; Prada, D. Monitoring photo-oxidation of the Prestige's oil spill by attenuated total reflectance infrared spectroscopy. *Talanta* **2006**, *69* (2), 409−417.
(27) Sharma, B. K.; Sarowha, S. L. S.; Bhagat, S. D.; Tiwari, R. K.; Gupta, S. K.; Venkataramani, P. S. Hydrocarbon group type analysis of petroleum heavy fractions using the TLC−FID technique. *Fresenius J. Anal. Chem.* **1998**, *360* (5), 539−544.
(28) Barman, B. N.; Cebolla, V. L.; Membrado, L. Chromatographic techniques for petroleum and related products. *Crit. Rev. Anal. Chem.* **2000**, *30*, 75−120.
(29) Reddy, C. M.; DeMello, J. A.; Carmichael, C. A.; Peacock, E. E.; Xu, L.; Arey, J. S. Determination of biodiesel blending percentages using natural abundance radiocarbon analysis: Testing the accuracy of retail biodiesel blends. *Environ. Sci. Technol.* **2008**, *42* (7), 2476−2482.
(30) Ventura, G. T.; Raghuraman, B.; Nelson, R. K.; Mullins, O. C.; Reddy, C. M. Compound class oil fingerprinting techniques using comprehensive two-dimensional gas chromatography (GC×GC). *Org. Geochem.* **2010**, *41* (9), 1026−1035.
(31) Mitra, S.; Kimmel, D. G.; Snyder, J.; Scalise, K.; McGlaughon, B. D.; Roman, M. R.; Jahn, G. L.; Pierson, J. J.; Brandt, S. B.; Montoya, J. P.; Rosenbauer, R. J.; Lorenson, T. D.; Wong, F. L.; Campbell, P. L., Macondo-1 well oil-derived polycyclic aromatic hydrocarbons in mesozooplankton from the northern Gulf of Mexico. *Geophys. Res. Lett.* **2012**, *39*, (1).
(32) Wang, Z. D.; Fingas, M. Fate and identification of spilled oils and petroleum products in the environment by GC-MS and GC-FID. *Energy Sources* **2003**, *25* (6), 491−508.
(33) Prince, R. C.; Elmendorf, D. L.; Lute, J. R.; Hsu, C. S.; Haith, C. E.; Senius, J. D.; Dechert, G. J.; Douglas, G. S.; Butler, E. L. 17α(*H*),21β(*H*)-hopane as a conserved internal marker for estimating the biodegradation of crude oil. *Environ. Sci. Technol.* **1994**, *28* (1), 142−145.
(34) Kroll, J. H.; Donahue, N. M.; Jimenez, J. L.; Kessler, S. H.; Canagaratna, M. R.; Wilson, K. R.; Altieri, K. E.; Mazzoleni, L. R.; Wozniak, A. S.; Bluhm, H.; Mysak, E. R.; Smith, J. D.; Kolb, C. E.; Worsnop, D. R. Carbon oxidation state as a metric for describing the chemistry of atmospheric organic aerosol. *Nat. Chem.* **2011**, *3* (2), 133−139.
(35) Slater, G. F.; Nelson, R. K.; Kile, B. M.; Reddy, C. M. Intrinsic bacterial biodegradation of petroleum contamination demonstrated in situ using natural abundance, molecular-level C-14 analysis. *Org. Geochem.* **2006**, *37* (9), 981−989.
(36) Haddad, R. I.; Martens, C. S.; Farrington, J. W. Quantifying early diagenesis of fatty acids in a rapidly accumulating coastal marine sediment. *Org. Geochem.* **1992**, *19* (1−3), 205−216.
(37) Atlas, R. M. Microbial degradation of petroleum hydrocarbons: an environmental perspective. *Microbiol. Rev.* **1981**, *45* (1), 180−209.
(38) Prince, R. C.; Garrett, R. M.; Bare, R. E.; Grossman, M. J.; Townsend, T.; Suflita, J. M.; Lee, K.; Owens, E. H.; Sergy, G. A.; Braddock, J. F.; Lindstrom, J. E.; Lessard, R. R. The roles of photooxidation and biodegradation in long-term weathering of crude and heavy fuel oils. *Spill Sci. Technol. Bull.* **2003**, *8* (2), 145−156.
(39) Leblond, J. D.; Schultz, T. W.; Sayler, G. S. Observations on the preferential biodegradation of selected components of polyaromatic hydrocarbon mixtures. *Chemosphere* **2001**, *42* (4), 333−343.
(40) Lima, A. L. C.; Farrington, J. W.; Reddy, C. M. Combustion-derived polycyclic aromatic hydrocarbons in the environment—A review. *Environ. Forensics* **2005**, *6* (2), 109−131.
(41) Jones, D.; Scarlett, A. G.; West, C. E.; Rowland, S. J. Toxicity of individual naphthenic acids to *Vibrio fischeri*. *Environ. Sci. Technol.* **2011**, *45* (22), 9776−9782.
(42) Vrabie, C. M.; Sinnige, T. L.; Murk, A. J.; Jonker, M. T. O. Effect-directed assessment of the bioaccumulation potential and chemical nature of Ah receptor agonists in crude and refined oils. *Environ. Sci. Technol.* **2012**, *46* (3), 1572−1580.
(43) Lübcke-von Varel, U.; Machala, M.; Ciganek, M.; Neca, J.; Pencikova, K.; Palkova, L.; Vondracek, J.; Löffler, I.; Streck, G.; Reifferscheid, G.; Flückiger-Isler, S.; Weiss, J. M.; Lamoree, M.; Brack, W. Polar compounds dominate in vitro effects of sediment extracts. *Environ. Sci. Technol.* **2011**, *45* (6), 2384−2390.
(44) Incardona, J. P.; Vines, C. A.; Anulacion, B. F.; Baldwin, D. H.; Day, H. L.; French, B. L.; Labenia, J. S.; Linbo, T. L.; Myers, M. S.; Olson, O. P.; Sloan, C. A.; Sol, S.; Griffin, F. J.; Menard, K.; Morgan, S. G.; West, J. E.; Collier, T. K.; Ylitalo, G. M.; Cherr, G. N.; Scholz, N. L. Unexpectedly high mortality in Pacific herring embryos exposed to the 2007 *Cosco Busan* oil spill in San Francisco Bay. *Proc. Natl. Acad. Sci. U.S.A.* **2012**, *109* (2), E51−E58.
(45) Incardona, J. P.; Vines, C. A.; Linbo, T. L.; Myers, M. S.; Sloan, C. A.; Anulacion, B. F.; Boyd, D.; Collier, T. K.; Morgan, S.; Cherr, G. N.; Scholz, N. L. Potent phototoxicity of marine bunker oil to translucent herring embryos after prolonged weathering. *PLoS One* **2012**, *7* (2), e30116.
(46) Di Toro, D. M.; McGrath, J. A.; Stubblefield, W. A. Predicting the toxicity of neat and weathered crude oil: Toxic potential and the toxicity of saturated mixtures. *Environ. Toxicol. Chem.* **2007**, *26* (1), 24−36.

(47) Hsu, C. S.; Hendrickson, C. L.; Rodgers, R. P.; McKenna, A. M.; Marshall, A. G. Petroleomics: Advanced molecular probe for petroleum heavy ends. *J. Mass Spectrom.* **2011**, *46* (4), 337−343.
(48) Klein, G. C.; Angstrom, A.; Rodgers, R. P.; Marshall, A. G. Use of saturates/aromatics/resins/asphaltenes (SARA) fractionation to determine matrix effects in crude oil analysis by electrospray ionization Fourier transform ion cyclotron resonance mass spectrometry. *Energy Fuels* **2006**, *20* (2), 668−672.